

## Human p8 Is a HMG-I/Y-like Protein with DNA Binding Activity Enhanced by Phosphorylation\*

Received for publication, September 20, 2000, and in revised form, October 26, 2000  
Published, JBC Papers in Press, October 30, 2000, DOI 10.1074/jbc.M008594200

José A. Encinar,<sup>a,b,c</sup> Gustavo V. Mallo,<sup>b,d,k</sup> Cynthia Mizyrycki,<sup>e,f</sup> Luciana Giono,<sup>e</sup>  
José M. González-Ros,<sup>a,c</sup> Manuel Rico,<sup>g</sup> Eduardo Cánepa,<sup>e,h</sup> Silvia Moreno,<sup>e,h</sup> José L. Neira,<sup>a,i</sup>  
and Juan L. Iovanna,<sup>a,i,j</sup>

From the <sup>a</sup>Centro de Biología Molecular y Celular, Universidad Miguel Hernández, 03202, Elche, Alicante, Spain, the <sup>d</sup>Unit 315 INSERM, 46 Boulevard de la Gaye, 13009 Marseille, France, the <sup>e</sup>Departamento de Química Biológica, Facultad de Ciencias Exactas y Naturales, Universidad de Buenos Aires, Ciudad Universitaria, 1428 Buenos Aires, Argentina, and the <sup>g</sup>Instituto de Estructura de la Materia (Consejo Superior de Investigaciones Científicas), Serrano 119, 28006 Madrid, Spain

We have studied the biochemical features, the conformational preferences in solution, and the DNA binding properties of human p8 (hp8), a nucleoprotein whose expression is affected during acute pancreatitis. Biochemical studies show that hp8 has properties of the high mobility group proteins, HMG-I/Y. Structural studies have been carried out by using circular dichroism (near- and far-ultraviolet), Fourier transform infrared, and NMR spectroscopies. All the biophysical probes indicate that hp8 is monomeric (up to 1 mM concentration) and partially unfolded in solution. The protein seems to bind DNA weakly, as shown by electrophoretic gel shift studies. On the other hand, hp8 is a substrate for protein kinase A (PKA). The phosphorylated hp8 (PKAhp8) has a higher content of secondary structure than the non-phosphorylated protein, as concluded by Fourier transform infrared studies. PKAhp8 binds DNA strongly, as shown by the changes in circular dichroism spectra, and gel shift analysis. Thus, although there is not a high sequence homology with HMG-I/Y proteins, hp8 can be considered as a HMG-I/Y-like protein.

The human p8 protein, hp8, is expressed at very low levels in the healthy pancreas, whereas it is highly expressed during the acute phase of pancreatitis and minor pancreatic injuries (1, 2). Further experiments showed that p8 mRNA expression is not restricted to the pancreatic cells, because p8 mRNA is also activated in several tissues in response to a systemic lipopolysaccharide injection (3). *In vitro*, p8 mRNA is expressed in

response to some pro-apoptotic agents in pancreatic and in nonpancreatic derived cells (1). The mechanism of gene activation is not clearly established, but the intracellular level of the CAAT enhancer-binding protein transcription factor seems to play a key role in its activation because the hp8 promoter activity is directly related to the CAAT enhancer-binding protein intracellular concentration (2). These observations indicate that hp8 is, in fact, activated in response to several cellular injuries and its overexpression seems to be cell type-independent.

Although the exact function of hp8 is unknown, preliminary results suggest that it could act as a cellular growth factor when overexpressed in some cellular lines (1, 2). Theoretical analysis of the hp8 sequence has shown a potential signal for nuclear targeting (1). This presumption was recently confirmed using specific antibodies and transient transfection of hp8 expression vectors (2). Sequence comparison in data bases did not identify proteins with homology to hp8, although it suggested the presence of a helix-loop-helix motif, characteristic of some families of DNA-interacting proteins (2, 4). Hp8 is also a phosphoprotein, although the sites of phosphorylation and the corresponding kinases are not known (2). Furthermore, a recent paper reports the cloning of the Com1 (candidate of metastasis 1) protein, which is identical to the hp8 mRNA, from human breast cancer cells with metastatic potential (5). hp8/Com1 seems to mediate the growth response of tumor cells upon the metastasis establishment in a secondary organ by an unknown mechanism (5).

Given its potential involvement in the cellular processes commented on above, it seems likely that the structural and thermodynamic characterization of hp8 could provide clues on new therapeutic strategies against pancreatitis and/or metastasis establishment or even its use as a new cellular growth factor. Here, we have carried out a structural characterization of a bacterially expressed His-tagged hp8 by using a four-part approach. First, we have compared p8 proteins from several species with HMG-I/Y proteins. Second, we have used several biophysical techniques, namely, CD, Fourier transform infrared (FTIR),<sup>1</sup> and NMR spectroscopies, to characterize hp8 structurally under different environments. Third, we have in-

\* The costs of publication of this article were defrayed in part by the payment of page charges. This article must therefore be hereby marked "advertisement" in accordance with 18 U.S.C. Section 1734 solely to indicate this fact.

<sup>b</sup> These authors contributed equally to this work.

<sup>c</sup> Supported by the Project DGESIC, PM 98-0098 of the Spanish Ministerio de Educación y Cultura.

<sup>f</sup> Graduate fellow from Consejo Nacional de Investigaciones Científicas y Técnicas (CONICET).

<sup>h</sup> Supported by grants from CONICET and Agencia Nacional de Promoción Científica y Tecnológica.

<sup>i</sup> To whom correspondence may be addressed: Centro de Biología Molecular y Celular, Universidad Miguel Hernández, 03202 Elche, Alicante, Spain. Tel.: 34-966658459; Fax: 34-966658758; E-mail: jneira@umh.es.

<sup>j</sup> Supported by La Ligue de Lutte contre le Cancer. To whom correspondence may be addressed: Unit 315 INSERM, 46 Bd. de la Gaye, 13009 Marseille, France. Tel.: 33-491172176; Fax: 33-491266219; E-mail: iovanna@marseille.inserm.fr.

<sup>k</sup> Supported by Humboldt Foundation.

<sup>1</sup> The abbreviations used are: FTIR, Fourier transform infrared; TFE, (2,2,2)-trifluoroethanol; TSP, 3-(trimethylsilyl) propionic acid-2,2,3,3-<sup>2</sup>H<sub>4</sub>-sodium salt; PAGE, polyacrylamide gel electrophoresis; MOPS, 4-morpholinepropanesulfonic acid; CAPS, 3-(cyclohexylamino)propanesulfonic acid; EMSA, electrophoretic mobility shift assay; HMG, high mobility group; TCA, trichloroacetic acid; PKA, protein kinase A; Cdc2k, cyclin-dependent kinase cdc2; Tricine, N-[2-hydroxy-1,1-bis(hydroxymethyl)ethyl]glycine.



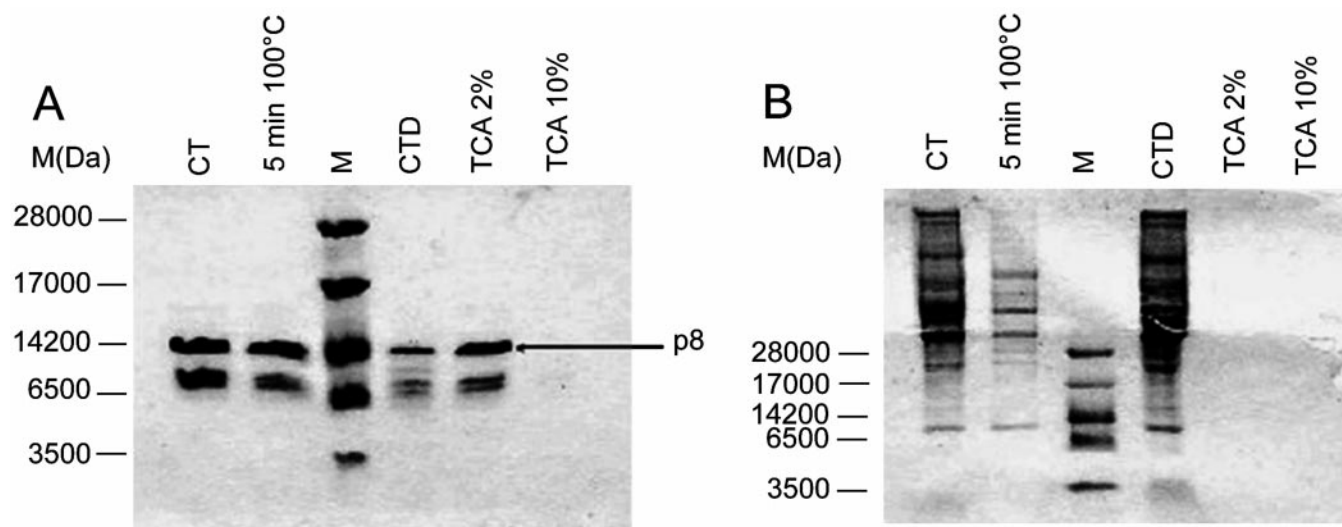


FIG. 2. **hp8 properties and thermal stability and sensitivity to precipitation by TCA.** A, Tris-Tricine 16.5% SDS-PAGE gel followed by Coomassie Brilliant Blue G staining of the following samples: Lane M, molecular mass markers; lane CT, control of 6  $\mu$ g of purified hp8; lane 5 min 100  $^{\circ}$ C, 6  $\mu$ g of hp8 heated at 100  $^{\circ}$ C for 5 min followed by centrifugation and loading of the supernatant; lane CTD, 4  $\mu$ g of hp8 centrifuged and the supernatant dialyzed and loaded into the gel (control to the TCA 2% lane); lane TCA 2%, 4  $\mu$ g of hp8 treated with TCA 2% and centrifuged and the dialyzed supernatant loaded into the gel; lane TCA 10%, 4  $\mu$ g of hp8 treated with TCA 10% and centrifuged and the dialyzed supernatant loaded into the gel. B, the same as in A, but using 23  $\mu$ g of HeLa crude extract for comparison, submitted to the same treatments as hp8. In the figure hp8 is indicated as p8.

tration was 20–30  $\mu$ M. Samples were prepared ranging from 2 to 80% (in volume) of the cosolvent, in buffer phosphate, pH 6.0, 2 mM NaCl and left overnight to equilibrate. None of the samples showed aggregation or precipitation after this time. A 0.1-cm-pathlength cell was used. Spectra were acquired at a scan speed of 50 nm/min, and six scans were recorded. The response time was 2 s.

GdmCl titrations were carried out in the same buffer (pH 6.0, 2 mM NaCl) by dissolving the proper amount of the denaturant from an 8 M stock solution and left overnight to equilibrate. Spectra were acquired at a scan speed of 50 nm/min, and six scans were recorded. The response time was 2 s. Cells with a pathlength of 0.1 cm, and a protein concentration 20–30  $\mu$ M were used for these experiments. The changes in the presence of  $\text{Na}_2\text{SO}_4$  (0–1 M) and pH (2.5–8.5) were also observed in an identical manner. Spectra were corrected by subtracting the base line in all cases.

The helical content of either phosphorylated or nonphosphorylated hp8 at any condition was approximated from its molar ellipticity at 222 nm (7).

$$f_h = [\Theta]_{222} / [\Theta]_{222}^{\infty} (1 - k/n) \quad (\text{Eq. 2})$$

where  $f_h$  is the helical fraction of the protein,  $[\Theta]_{222}$  is the observed mean residue ellipticity,  $[\Theta]_{222}^{\infty}$  is the mean ellipticity for an infinite helix at 222 nm ( $-34,500 \text{ deg cm}^2 \text{ dmol}^{-1}$ ),  $k$  is a wavelength-dependent constant (2.57 at 222 nm), and  $n$  is the number of peptide bonds (92 for hp8).

**Fourier Transform Infrared Spectroscopy**—The protein was lyophilized and dissolved in deuterated buffer, containing 10 mM MOPS, 10 mM CAPS, 10 mM sodium acetate buffer, 0.1 mM EDTA, 100 mM NaCl. Samples of hp8 at a final concentration of 10 mg/ml were placed in a Harrick Ossining demountable cell. Spectra were acquired on a Nicolet 520 instrument equipped with a deuterated triglycine sulfate detector and thermostated with a water bath at 20 ( $\pm 0.1$ )  $^{\circ}$ C. The cell container was continuously filled with dry air. Usually, 600 scans/sample were taken, averaged, apodized with a Happ-Genzel function, and Fourier-transformed to give a resolution of 2  $\text{cm}^{-1}$ . Contribution of buffer spectra was subtracted, and the resulting spectra were used for analysis, after smoothing. Spectra smoothing was carried out applying the maximum entropy method, assuming that noise and band shape follow a normal distribution. The minimum bandwidth was set to 12  $\text{cm}^{-1}$  (8). The signal/noise ratio of the processed spectra was better than 11000:1. Derivation of IR spectra was performed using a power of 3, breakpoint of 0.3; Fourier self-deconvolution was performed using a Lorentzian bandwidth of 18  $\text{cm}^{-1}$  and a resolution enhancement factor of 2.0 (9–11). Experiments were acquired at pD (pH in deuterated water as measured by pH meter) 3.9, 6.9, and 10.9 to detect possible changes in the structure. The pH measurements were corrected from the pH meter reading, according to:  $\text{pH} = \text{pH}_{\text{read}} + 0.4$ .

Protein secondary structure was quantified by band deconvolution of the amide I band (8, 12). The number and position (wave number) of the bands were taken from the deconvoluted spectra; the bandwidth was estimated from the derived spectra; and the height band taken from raw spectra (13). The iterative curve-fitting process was performed in CURVEFIT running under SpectraCalc (Galactic Industries Corp., Salem, NH). The number, position, and band shape were fixed during the first 200 iterations. The fitting was further refined by allowing the band positions to vary for 50 additional iterations. The goodness of the fit was assessed from the  $\chi^2$  values ( $4 \times 10^{-5}$  to  $6.5 \times 10^{-5}$ ). The area of the fitted band was used to calculate the percentage of secondary structure (8, 14).

**Nuclear Magnetic Resonance Spectroscopy**— $^1\text{H}$  NMR experiments were carried out in a Bruker AMX-600 spectrometer at 5, 20, 25, and 30 ( $\pm 0.1$ )  $^{\circ}$ C with 32,000 data points and using presaturation to eliminate the water signal. Typically, 1024 scans were acquired in each sample. The spectral width was 6000 Hz in all cases. The buffer was the same used in the CD experiments. Exchange samples were prepared by dissolving a lyophilized aliquot in 500  $\mu$ l of precooled exchange buffer. To discard any artifact caused by unfolded protein from freeze drying, the sample in water was diluted 10 times in deuterated water, and the spectrum was recorded and compared with that obtained previously. Both spectra were identical (data not shown). Spectra in aqueous solution were acquired at different concentrations of hp8, ranging from 0.1 to 1.5 mM. No changes in chemical shifts or line broadening were observed in any case.

Experiments in TFE were prepared by dissolving the lyophilized sample, in 60%:40% (TFE/water, volume/volume). The solutions in all cases were centrifuged briefly to remove insoluble protein and then transferred to a 5-mm NMR tube. Sample concentrations were in all cases 1–1.5 mM. The TFE and exchange experiments were carried out with freshly prepared sample.  $^1\text{H}$  chemical shifts were quoted relative to TSP.

The spectra were processed using BRUKER-UXNMR software working on a SGI work station. Spectra were processed using an exponential window functions. Polynomial base-line corrections were applied. The final one-dimensional data contained 32,000 data points.

**DNA Binding Experiments Measured by Circular Dichroism**—The DNA binding experiments were carried out by mixing DNA (Type 1 Sigma from calf thymus) and the corresponding form of hp8 to give the required final concentration rate (weight/weight of protein/DNA) in phosphate buffer, pH 7, at 25 ( $\pm 0.1$ )  $^{\circ}$ C, and no salt. This pH was chosen to map DNA binding because it is close to physiological conditions, and no changes were observed in the shape of the CD spectra with pH (see “Results”). To avoid solution viscosity, DNA was sonicated on ice using short bursts. Experiments were carried out at a 1:1 concentration.

**DNA Binding Experiments Measured by Electrophoretic Mobility**

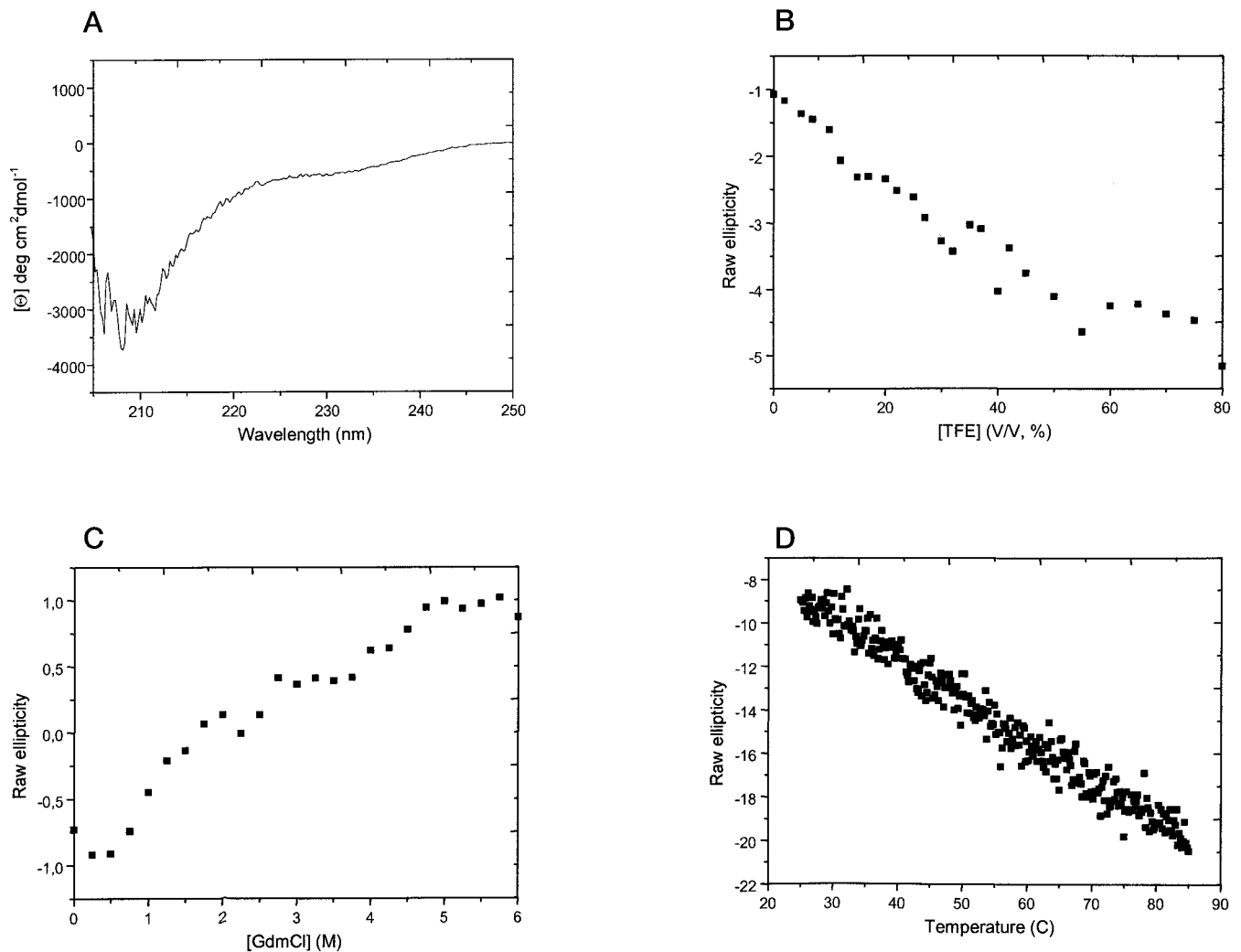


FIG. 3. **Secondary structure analyzed through circular dichroism.** A, far-UV circular dichroism spectrum of the hp8. B, TFE titration by observation of raw ellipticity at 222 nm. C, GdmCl denaturation by following the raw ellipticity at 222 nm (similar results were obtained at 230 nm; data not shown). D, thermal denaturation of hp8 monitored by following the ellipticity at 222 nm. The conditions were 20  $\mu$ M of protein in phosphate buffer, pH 6, 2 mM NaCl at  $25 \pm 0.1$  °C (except for D); spectra were acquired in a 0.1-cm-pathlength cell.

**Shift Assay**—For the gel retardation assays, the double-stranded oligonucleotide corresponding to positions 37–57 (ATGCCACCTGCCACCAACA) from *Mus musculus* p8 mRNA (AF131196) was used. The oligonucleotide was end-labeled, using [ $\gamma$ - $^{32}$ P]dATP (3000 Ci/mmol) and T4 polynucleotide kinase, and purified by MicroSpin G-25 columns (Amersham Pharmacia Biotech). The DNA probe (50,000–200,000 cpm) was incubated for 30 min at room temperature with purified hp8 protein as indicated in each experiment. Reactions were carried out in a final volume of 30  $\mu$ l containing 25 mM Hepes-KOH, pH 7.9, 50 mM NaCl, 1 mM dithiothreitol, 0.05% Nonidet P-40, 10% glycerol, and 0.5  $\mu$ g of acetylated bovine serum albumin. In competition experiments, the protein was first incubated 15 min in binding buffer with the indicated excess of the unlabeled oligonucleotide before the addition of the labeled DNA. Samples were analyzed by electrophoresis at constant current (180 V) for ~2 h in nondenaturing 5% polyacrylamide gels in 0.5 $\times$  TBE (44.5 mM Tris, 44.5 mM borate, 1 mM EDTA). Gels were dried and exposed overnight to X15 Kodak films.

## RESULTS

### hp8 Has Characteristics of HMG-I/Y Proteins

hp8 is 82 amino acids long, showing an overall identity of around 75% with its mouse and rat counterparts (Fig. 1A). Inspection and analysis of the sequences shows some interesting features: a high isoelectric point (9.6–10.4), 14% of acidic amino acids, 20–24% of basic amino acids, 14–17% of phosphorylatable amino acids (serine, threonine, and tyrosine), and a high abundance of proline (6–9%) and glycine (5–6%). The

negative charged residues appear located at the amino-terminal region, and all the positive residues accumulate in the carboxyl-terminal region (Fig. 1A). All of these features are similar to those shown by some high mobility group (HMG) proteins (15), particularly by the HMG-I/Y family (Fig. 1B). The overall identity of hp8 with human HMG-I/Y is only around 35%, but the molecular mass, isoelectric point, the percentage of Arg + Lys, Glu + Asp, Ser + Thr, Gly + Pro, hydrophilicity plot, and charge separation (despite a reverse orientation) are very similar. A characteristic property of these HMG proteins is that they are not denatured by heating at 100 °C; further, they are not precipitated by 2% trichloroacetic acid (TCA). We analyzed these two properties on a purified preparation of recombinant His-hp8. Fig. 2A shows that His-hp8 is resistant to heat denaturation and is recovered from the supernatant of 2% TCA precipitation, although it is precipitated by 10% TCA. The apparent molecular mass of 14 kDa of the recombinant protein on SDS gel is higher than the theoretical molecular mass of 10.1 kDa, very probably because of the highly charged nature of the protein (16). Fig. 2B shows a control experiment using a mixture of proteins from a cell extract (using, for the example, a crude extract from HeLa cells); only few proteins resist heat denaturation, and all the proteins are precipitated by 2% TCA.

A

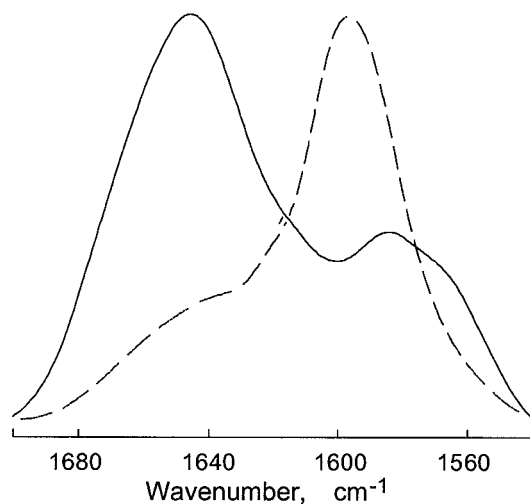
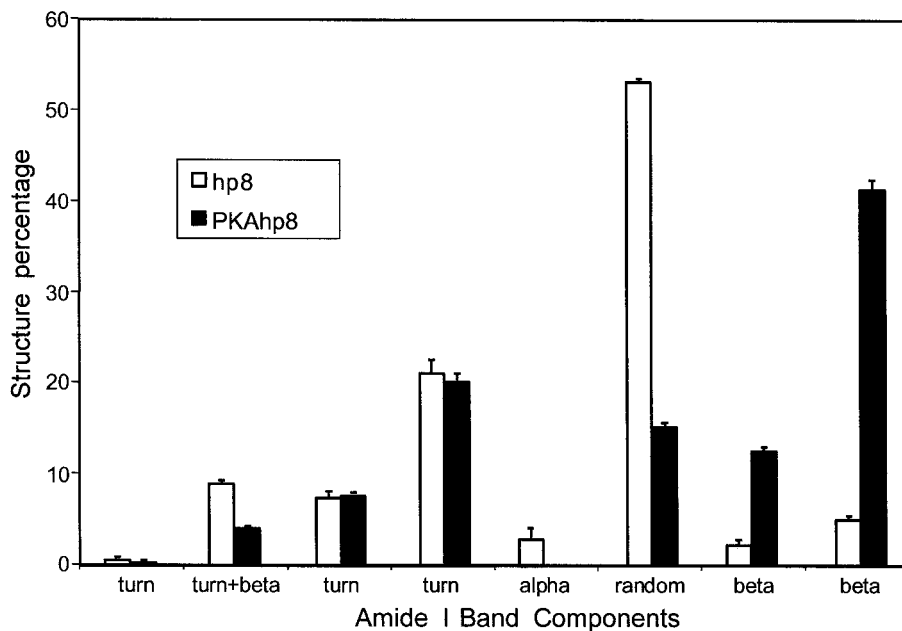


FIG. 4. FTIR spectra in the 1700–1540  $\text{cm}^{-1}$  region. A, nonphosphorylated (continuous line), and PKAhp8 protein (dotted line). B, calculated percentages of the secondary structure in the nonphosphorylated (empty bars) and phosphorylated samples (black bars). Secondary structure elements were calculated by band decomposition and curve fitting of the original amide I band after spectra smoothing (see “Experimental Procedures”). The pD was 6.9, and the temperature was  $20 \pm 0.1$  °C.

B



#### Structural Studies of the Nonphosphorylated hp8

HMG-I/Y proteins are unfolded in solution. The similarity of hp8 to this family of proteins and its composition of amino acids that does not favor secondary structure (high content of Gly and Pro and low content of hydrophobic amino acids) prompted us to analyze the structural properties of hp8.

#### Circular Dichroism Spectroscopy

**Far-UV Spectrum**—The far-UV spectrum reflects primarily the conformation of the protein backbone and hence the content of secondary structure. The spectrum of hp8 at pH 6.0 and 25 °C displays an intense minimum at 205 nm (Fig. 3A) and a shoulder expanding from 220 to 230 nm. Such spectrum resembles, except for the shoulder, that of a random coil structure (17, 18). The spectrum was invariable in the pH range 2.0–8.5 (data not shown). No turbidity was observed when the pH was close to the theoretical isoelectric point ( $\text{pI} = 10.19$ ). It is common to use the ellipticity at 222 nm as a measure of the

helical secondary structure of a protein (Equation 2). The percentage of calculated structure is 2%. Thus, hp8 from the far-UV spectra is mainly random coil.

Addition of either  $\text{Na}_2\text{SO}_4$  or SDS decreased the CD signal at 222 nm (data not shown). In both cases, the general shape of the spectra did not change when compared with that acquired in aqueous solution.

The ellipticity at 222 nm decreased continuously upon addition of TFE up to a concentration of 60% (volume/volume), where the titration curve reached a saturation phase and remained constant (Fig. 3B). In 60% TFE (Equation 2), the percentage of helical structure is 9%.

The ellipticity increased (more positive) monotonically as concentration of guanidinium hydrochloride ([GdmCl]) was raised (Fig. 3C), indicating that the denaturation is a noncooperative process. The spectra at high [GdmCl] showed a positive band around 220 nm, as it should be expected in completely random coil proteins (18). These findings suggest that the 222

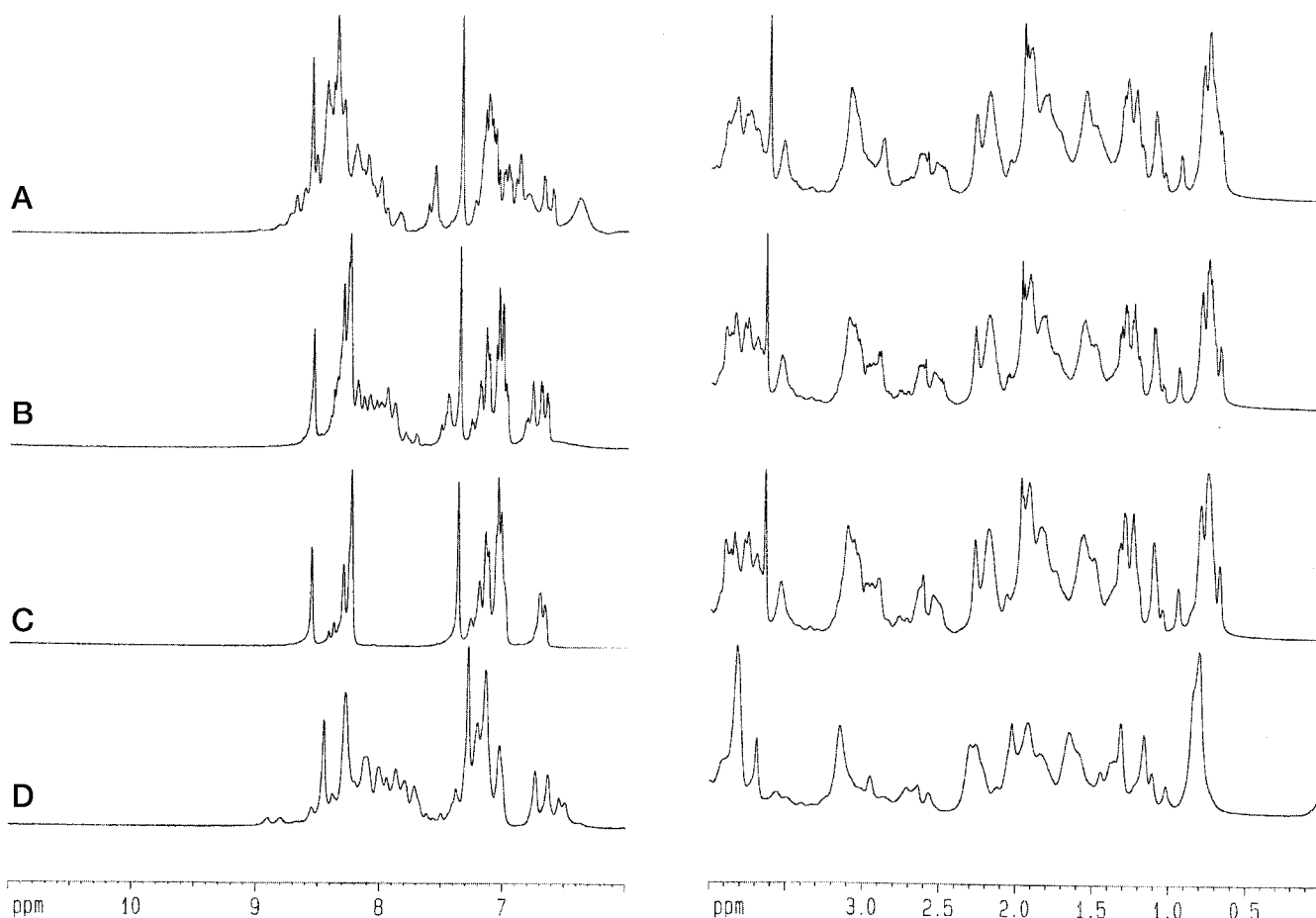


FIG. 5. Tertiary and secondary structure changes in hp8 as mapped by one-dimensional NMR. Amide (left side) and methyl (right side) region of nonphosphorylated protein. A, pH 6.0 in phosphate buffer, 2 mM NaCl, at  $5 \pm 0.1$  °C. B, pH 6.0 in phosphate buffer, 2 mM NaCl, at  $25 \pm 0.1$  °C. C, hydrogen-deuterium exchange after 5 min of incubation in deuterated water at  $25 \pm 0.1$  °C, in phosphate buffer (pH 6.0), 2 mM NaCl. D, pH 6.0 in phosphate buffer, 2 mM NaCl, 60% TFE at  $25 \pm 0.1$  °C.

nm band, under native conditions, could indicate partially folded conformations, although the general shape of the spectra correspond to random coil conformations.

**Near-UV Spectrum**—The near-UV spectrum provides information on the asymmetry of the environment of aromatic residues and therefore on tertiary structural features. The near-UV signal of hp8 was null at pH 6.0 and did not change with either the pH or temperature, suggesting the absence of a well fixed structure. No changes were observed in this region upon addition of SDS,  $\text{Na}_2\text{SO}_4$ , TFE, or GdmCl (data not shown).

The lack of a well fixed tertiary structure was also confirmed by fluorescence studies. The fluorescence spectrum of hp8 shows exposed tyrosine residues, with a maximum at 305 nm (data not shown).

**Thermal Denaturation**—The thermal denaturation of hp8 at pH 6.0 is linear with temperature. This indicates the absence of cooperativity, as expected for a noncompact structure (Fig. 3D). Similar results were obtained at pH 4.0 and pH 7.0 (data not shown).

#### Fourier Transform Infrared Spectroscopy

In the case of proteins, structural information can be obtained by analyzing the amide I region of the spectrum ( $1700\text{--}1600\text{ cm}^{-1}$ ). The absorbance in this band region is predominantly due to the stretching vibration of the carbonyl peptide bond, whose frequency is highly sensitive to hydrogen bonding and thus to protein secondary structure (19). Representative FTIR spectra of nonphosphorylated human hp8 and PKA phosphorylated hp8 (see below) samples are shown in Fig. 4. The

infrared spectrum of nonphosphorylated hp8 (Fig. 4A) showed an amide I band with a maximum centered near  $1644\text{ cm}^{-1}$ , which is characteristic of nonordered conformations. Amide I band analysis by self-deconvolution showed maxima centered at 1690, 1679, 1670, 1660, 1649, 1641, 1635, and  $1612\text{ cm}^{-1}$ . The  $1612\text{ cm}^{-1}$  component corresponds to amino acid side chain vibration, and the other maxima are assigned to vibration of peptide carbonyl groups involved in different secondary structural motifs (20). The  $1635\text{ cm}^{-1}$  is assigned to  $\beta$ -sheet structure; the  $1641\text{ cm}^{-1}$  is assigned to nonordered structure; the  $1649\text{ cm}^{-1}$  component is assigned to  $\alpha$ -helix; the  $1660\text{ cm}^{-1}$  is assigned to helical  $3_{10}$  structure; the  $1690$  and  $1670\text{ cm}^{-1}$  components are assigned to turns; and the  $1679\text{ cm}^{-1}$  band includes contributions from turns as well as from the  $(0, \pi)$   $\beta$ -sheet vibration band (21, 22). The percentage of secondary structure calculated from the area of the fitted bands is represented in Fig. 4B. The nonphosphorylated hp8 showed a 53% content of nonordered structure.

#### Nuclear Magnetic Resonance Spectroscopy

NMR can give information about the general topology of the polypeptide chain in solution. The  $^1\text{H}$  atom is the observed nucleus in proteins, whose chemical shift depends on which atom it is bonded to and on its environment.

Experiments were acquired at low ( $5$  °C; Fig. 5A) and high temperatures ( $25$  °C; Fig. 5B) to check for possible temperature stabilization of structure, as it has been observed in some HMG proteins (23). The one-dimensional NMR spectra of human hp8 at  $5$  °C showed small chemical shift dispersion: the amide (Fig.

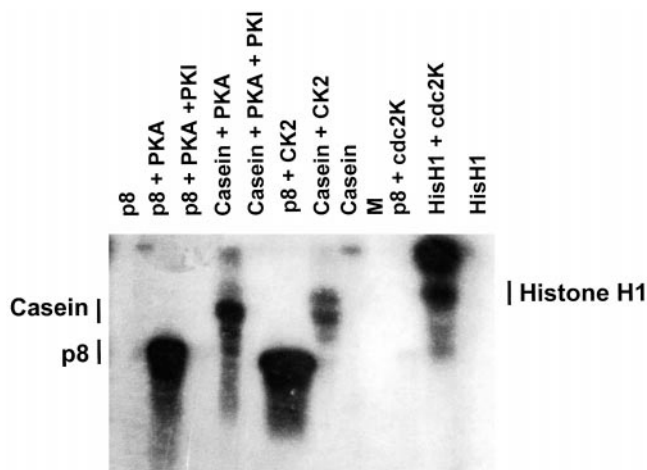


**FIG. 6. Phosphorylation of hp8 with several protein kinases.** 100  $\mu$ g of hp8 were submitted to phosphorylation in 50- $\mu$ l reaction mixtures, as indicated under "Experimental Procedures" by the following protein kinases: PKA, in the absence or presence of 1  $\mu$ M protein kinase A-specific thermostable peptide inhibitor (PKI), casein kinase 2 (CK2), and Cdc2k. Positive control reactions for phosphorylation by each kinase were performed with either casein or histone H1 (*HisH1*). One-fourth of each reaction mixture was loaded on 17.5% SDS-PAGE. Gels were run, dried, and radioautographed. *M* indicates the molecular mass markers. In the figure hp8 is indicated as *p8*.

5A, left) and the methyl (Fig. 5A, right) protons were clustered in those regions expected for random coil proteins (24). A similar spectrum was observed at 25  $^{\circ}$ C (Fig. 5B). At both temperatures, the line widths of protons of the amide region were not significantly broader than those of proteins with similar size. Signals between 7.5 and 8.5 ppm and between 6.0 and 7.0 ppm appeared at low temperatures. These signals must belong to the amide protons and the side chains of Arg, Asn, and Gln, which are now observed because of their slower exchange rates. Although the appearance of new signals in the methyl region was not observed at low temperature, signal narrowness at high temperatures allowed the clear distinction of a methyl proton at 0.68 ppm. It is interesting to note that this signal does not correspond to the expected random coil chemical shift for any methyl proton (24), and thus, it suggests the presence of nonrandom interactions.

In the hydrogen/deuterium exchange (Fig. 5C), all the amide protons disappeared within 5 min. Only the aromatic protons of the six-His tail, the two His in the sequence, the one Phe, and the two Tyr residues (Fig. 1) could be observed between 6.8 and 7.4 ppm and between 8.2 and 8.6 ppm. The fact that all the amide protons exchange so fast with solvent indicates that no stable hydrogen-bonded structure is present in hp8.

Experiments in the presence of 60% TFE (Fig. 5D) induced chemical shift dispersion and also signal broadening in the amide region. The methyl region remained invariable, except for the larger broadening. Furthermore, the two-dimensional nuclear Overhauser effect spectroscopy experiments showed lack of long-range contacts (data not shown), suggesting the absence of a well fixed tertiary structure.

#### Phosphorylation of hp8

The fact that hp8 has a high percentage of serines and threonines prompted us to assay the capacity of being phosphorylated by some of the protein kinases predicted to have putative target sites in hp8. Fig. 6 shows that protein kinase A (PKA) and casein kinase 2 phosphorylated hp8, but that Cdc2k did not. Casein was used as a positive control in phosphorylation by both PKA and casein kinase 2. Phosphorylation of hp8 and casein by PKA was inhibited by its thermostable specific

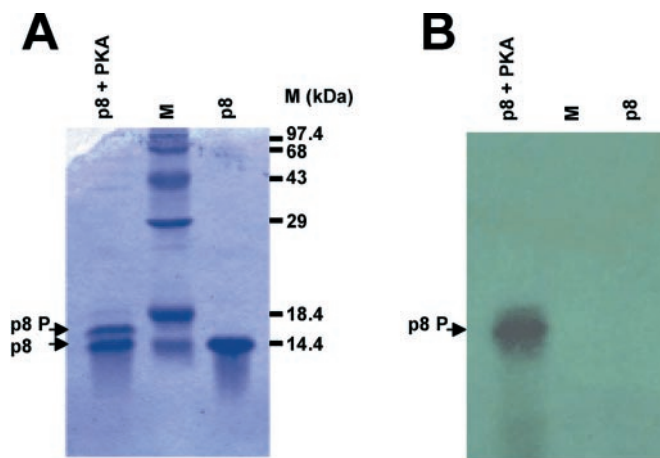


**FIG. 7. Phosphorylation of hp8 by PKA.** 100  $\mu$ g of hp8 were submitted to extensive phosphorylation by PKA by incubation during 180 min, as indicated under "Experimental Procedures." 10  $\mu$ g of phosphorylated or unphosphorylated hp8 were loaded on 17.5% SDS-PAGE gels. *M* indicates the molecular mass markers. In the figure hp8 is indicated as *p8*.

protein inhibitor. Histone H1 was used as a positive control in phosphorylation by Cdc2k kinase. Also, the tyrosine kinase sarcoma tyrosine kinase p60 was assayed; the results indicate that hp8 is substrate of this kinase (data not shown).

To check for structural changes in hp8 upon phosphorylation, we have chosen as model the phosphorylation by PKA. PKA phosphorylation was followed either by SDS-PAGE and radioautography when using [ $\gamma$ - $^{32}$ P]ATP as substrate (Fig. 7) or by FTIR spectroscopy when using unlabeled ATP (Fig. 8). Fluorescence spectroscopy was not attempted because the phosphorylation reaction requires small amounts of PKA, which are not removed from the reaction mixture, and could interfere with the measurements. Even at highly optimized phosphorylation conditions, only 30% of hp8 could be phosphorylated, assuming that one phosphate was incorporated per molecule; phosphorylation produced the typical shift in electrophoretic mobility of phosphorylated proteins (Fig. 7). When using unlabeled ATP, protein phosphorylation was checked by observing the 950–1300  $\text{cm}^{-1}$  band of the FTIR spectra (25). Monoanionic and dianionic phosphate monoesters give rise to bands at 1180 and 980  $\text{cm}^{-1}$ , respectively (Fig. 8).

#### Structural Studies of the PKAhp8

We have used CD and FTIR to check for structural changes in PKAhp8 upon phosphorylation. Fluorescence was not used because of the presence of PKA (see above).

#### Circular Dichroism Spectroscopy

The far- and near-UV spectra of PKAhp8 at pH 6.0 were identical to the ones observed in nonphosphorylated hp8 (data not shown).

#### Fourier Transform Infrared Spectroscopy

The PKAhp8 FTIR spectrum (Fig. 4A) showed an amide I band with a maximum close to 1645  $\text{cm}^{-1}$ . Self-deconvolution of this band showed an increase in two components at 1625 and 1635  $\text{cm}^{-1}$  that were not detected in nonphosphorylated hp8. These components can be assigned to  $\beta$ -sheet structure (22, 26). Phosphorylation decreased the percentage of random structure (Fig. 4B), when compared with the hp8. This decrease (from 53 to 15% in PKAhp8) is concomitant with an increase in the  $\beta$ -sheet structure. Thus, the FTIR observations seem to indicate that phosphorylation promotes a disorder to order transition in hp8.

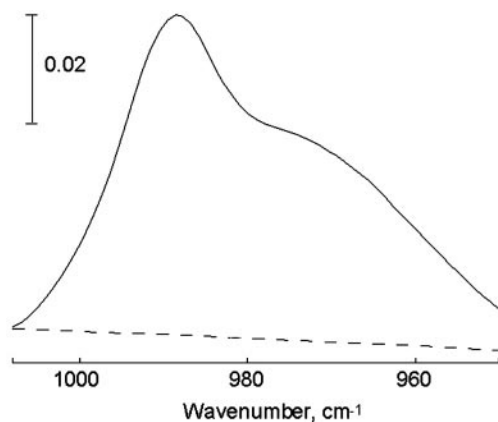


FIG. 8. PKA phosphorylation of hp8 by FTIR. FTIR studies of human hp8 showing the band assigned to the symmetric stretching of the dianionic phosphate monoester ( $950\text{--}1011\text{ cm}^{-1}$ ) in nonphosphorylated hp8 (dashed line) and protein kinase A phosphorylated hp8 (PKAhp8, continuous line). The protein concentration used was 1 mM. The freeze-dried sample was dissolved in  $\text{D}_2\text{O}$ -based buffer 10 mM MOPS, 10 mM CAPS, 10 mM sodium acetate buffer, pD 6.9, 0.1 mM EDTA, 100 mM NaCl,  $20 \pm 0.1^\circ\text{C}$ .

#### DNA Binding Properties of hp8 and PKAhp8

HMG-I/Y proteins belong to a new group of nuclear proteins referred to as “architectural transcription factors,” whose role in gene regulation is the recognition and modulation of both DNA and chromatin structure (15). These proteins recognize the narrow minor groove of A/T-rich target DNA rather than its nucleotide sequence. Because of the similarity in structure and properties of hp8 with this HMG family of proteins, we assayed whether it could interact with DNA, by using CD measurements and EMSA.

#### DNA Binding Explored by Circular Dichroism

DNA binding properties were explored in hp8 and PKAhp8 by using circular dichroism (18, 27). To check for DNA binding, we have compared the spectra of the putative complex (calf thymus DNA and hp8 or PKAhp8 in a 1:1 weight/weight ratio) versus the CD spectral composition resulting from adding the individual DNA and corresponding hp8 spectra. The comparison did not show changes when using nonphosphorylated hp8 either in the far-UV or near-UV, neither in the maxima, nor in the shape of the spectrum (Fig. 9A). There were, however, small changes in the spectra intensity. These results indicate that binding to DNA by the nonphosphorylated hp8, if any, is very weak.

However, addition of calf thymus DNA induced changes in the near and far-UV regions (Fig. 9B) of PKAhp8. The spectrum obtained after incubation of PKAhp8 and DNA together was different from that obtained by adding the spectra of both molecules separately. The maximum of the complex moved to shorter wavelengths, and the intensity of the spectrum of the complex was half-reduced. At 222 nm, the added spectrum showed a more negative ellipticity than that of the complex; conversely, in the region ranging from 225 to 240 nm, the spectrum of the complex showed a lower intensity than that of the added spectrum. These changes suggest that PKAhp8 binds DNA.

**DNA Binding Properties Explored by Gel Shift Assay**—We have also performed EMSA with radioactively labeled oligonucleotides containing different sequences and hp8 recombinant protein. Protein-DNA complexes were formed with similar efficiency on each oligonucleotide used (Fig. 10 and data not shown). These complexes were competed away in a concentration-dependent manner by the unlabeled oligonucleotide itself and

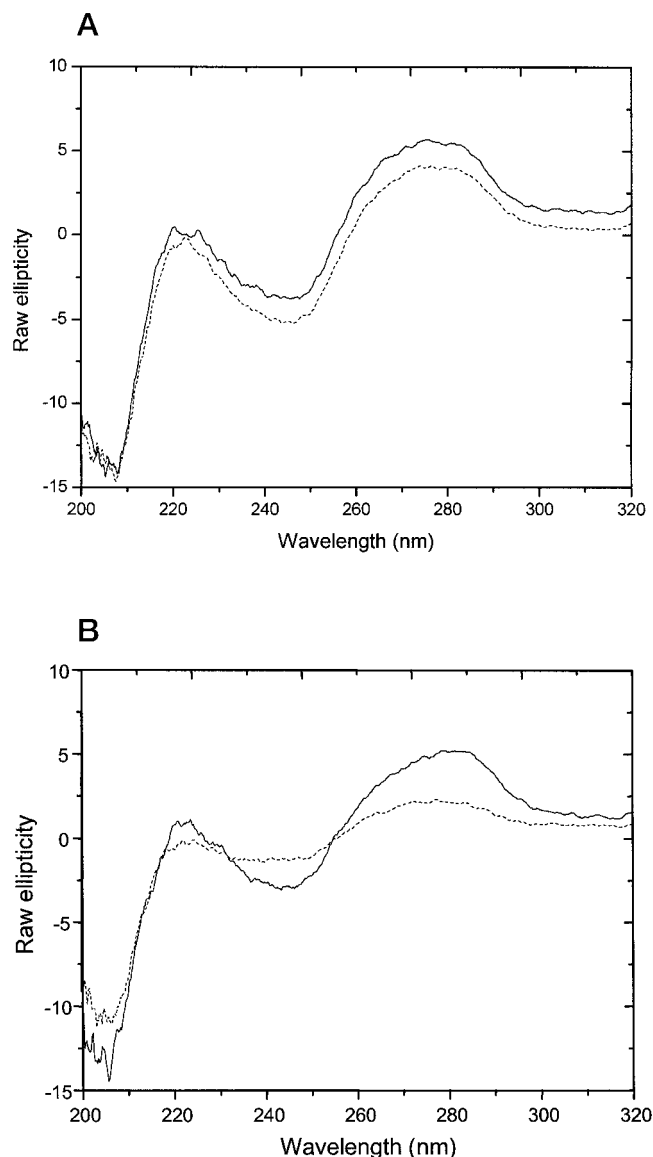


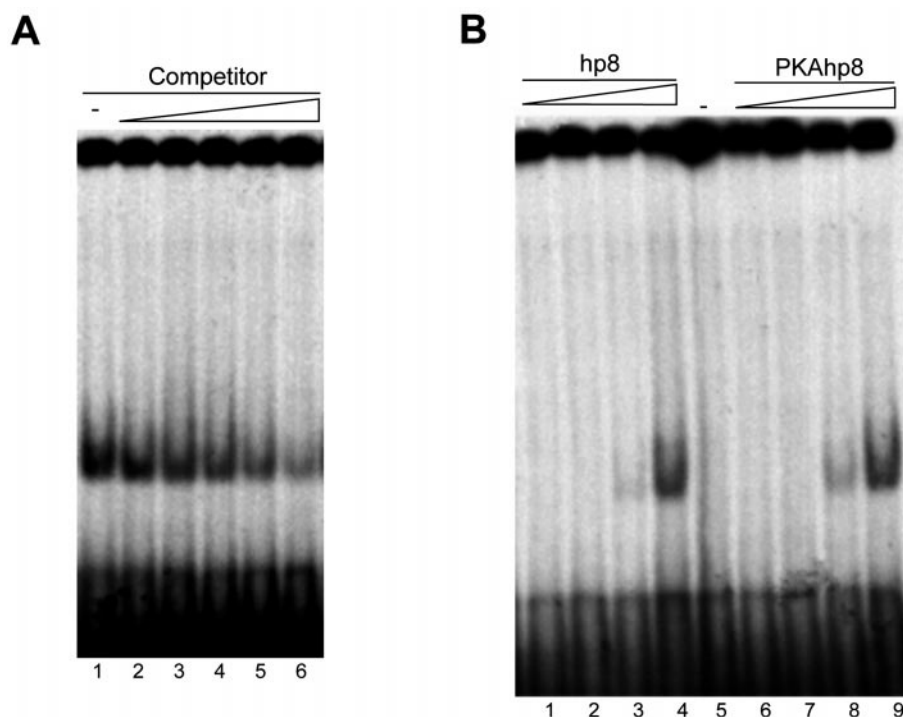
FIG. 9. DNA binding properties of nonphosphorylated hp8 and PKAhp8 mapped by CD experiments. A, CD spectral composition obtained by addition of the DNA and nonphosphorylated hp8 spectra (continuous line) and that obtained from the putative complex resulting by mixing the same amount (in grams) of DNA and nonphosphorylated hp8 (dashed line). B, CD spectral composition obtained by addition of the DNA and PKAhp8 spectra (continuous line) and that obtained from the putative complex resulting by mixing the same amount (in grams) of DNA and PKAhp8 (dashed line). The buffer used in both cases was 20 mM phosphate, pH 7, 2 mM NaCl; 0.2-cm-pathlength cells were used in all cases.

by the other DNA probes tested or poly(dI-dC) (Fig. 10A and data not shown). Having established that the hp8 binds to DNA, we sought to determine whether PKA-mediated phosphorylation of hp8 modified its DNA binding capacity. Fig. 10B shows that DNA binding activity was increased when hp8 recombinant protein was previously phosphorylated by PKA catalytic subunit. A rough estimate of 7-fold increase in affinity can be calculated from the increase in intensity of the complex at similar concentrations of hp8 and PKAhp8 proteins (around 2-fold) and the degree of phosphorylation of PKAhp8, which is around 30% (see before). Similar results were obtained with other oligonucleotides tested (data not shown).

#### DISCUSSION

**Conformational Preferences of the Nonphosphorylated hp8**—All the biophysical techniques show that hp8 lacks a well fixed

**FIG. 10. Binding of hp8 and PKAhp8 to DNA analyzed by EMSA.** *A*, EMSA was performed using hp8 protein and several oligonucleotides of double-stranded DNA as substrates. The results obtained with the oligonucleotide (ATGGCCACCTTGCCACAACA) are shown as an example. *Lane 1*, without competitor; *lanes 2–6*, increasing amounts of unlabeled oligonucleotide used as competitor: 4-, 8-, 16-, 32-, and 64-fold. *B*, increasing amounts of hp8 and PKAhp8 were assayed in EMSA using a double-stranded DNA as substrate (ATGGCCACCTTGCCACAACA). *i*, 0.1, 1, 3, and 6  $\mu\text{M}$  hp8; *lane 5*, no added hp8; *lanes 7–10*, 0.1, 1, 3, and 6  $\mu\text{M}$  PKAhp8.



tertiary structure, and it is, mainly, a random coil protein. This was further confirmed by the rapid hydrogen/deuterium exchange of the amide region (complete after 5 min; Fig. 5C). The lack of dispersion of the amide signals in the NMR and the absence of cooperativity during the thermal and chemical denaturation experiments (Fig. 3, C and D) also supports that the tertiary structure of hp8, if any, is very weak.

However, there is evidence of either residual secondary structure or local interactions. First, in the methyl region of the one-dimensional NMR spectra, there are protons whose chemical shifts are up-field shifted (Fig. 5, right); and second, far-UV CD spectra also show the presence of secondary structure as supported by the shoulder at 220 nm (Fig. 3A), which disappears at high denaturant concentrations (Fig. 3C). The origin of this band is unknown, but it could be due either to the presence of residual helical structure (2% as calculated by Equation 2) or to aromatic residues (18). Furthermore, FTIR experiments also predict the existence of either turn- or helix-like structures (Fig. 4B). There are, however, differences in the calculated percentage of secondary structure by CD and FTIR. Those differences could be due either to the deconvolution procedure (in the case of FTIR) or to the presence of aromatic residues, which affect the signal at 222 nm, in the case of CD (18). The presence of this residual structure seems to be consistent with the observation that TFE increases the percentage of secondary structure (28), going from 2% in aqueous solution to 9% in the final 60% TFE solution. However, those structures in 60% TFE are not involved in a well fixed structure, as shown by the almost complete lack of dispersion in the one-dimensional NMR spectra. This would agree with the proposed mechanism of action of alcohols on protein solutions, which strengthens local interactions but weakens long range ones (29). The populations of local folded conformations do not increase, however, by the presence of other agents. In conclusion, the evidence from the different techniques indicates that hp8 is essentially random coil in solution, although it contains weak and flickering secondary structure.

**Conformational Preferences of the PKAhp8**—The conformational changes detected in PKAhp8 when compared with hp8 are larger by FTIR than by CD, where the phosphorylated hp8

spectrum remains essentially unchanged. The possible reasons of this discrepancy have been described before. We favor the idea that the changes in the FTIR are due to true structural changes, which are not detected by CD; for example, in the CD spectra, the changes in the secondary structure (more  $\beta$ -sheet) could be hindered by the formation of  $\beta$ -turns, which show a positive band at 220 nm (18). It does not mean, however, that the percentages of assigned structures by FTIR (Fig. 4B) are reflecting the real content of secondary structure; rather, they must be taken as indicative of the structural changes involved.

**Disorder-Order Transition upon PKAhp8 Binding to DNA**—The changes in the near- and far-UV region of spectrum of PKAhp8 with DNA indicate binding to DNA. This interaction can only be accomplished if PKAhp8 suffers a disorder-order transition upon DNA binding, which has also been described in other proteins (23, 30, 31). This ordering, so far, has involved formation of  $\alpha$ -helices or quaternary rearrangements. In hp8, it seems that the DNA binding does not involve only formation of  $\alpha$ -helices, because the region about 222 nm lost its intensity (when compared with the addition spectrum; Fig. 9B). The transition must involve a complete rearrangement of the entire polypeptide chain, as concluded by (a) the changes between 225 and 240 nm, where  $\beta$ -turns can be detected by far-UV CD (18) and (b) the near-UV region, where tertiary structure around the aromatic chains is observed.

Apparently, there is a discrepancy between the CD and EMSA studies in the nonphosphorylated hp8 protein, because DNA binding is unambiguously indicated by the last technique. However, there is no contradiction between both results, because the CD measurements explored the DNA binding affinity when using the same amount in grams of hp8 and DNA; if the affinity was low, we should not expect large changes in the CD spectra. Conversely, the EMSA studies were done in a high excess of protein, and then the possible weak affinity is shifted toward complex formation.

However, why are the DNA binding properties enhanced upon phosphorylation? Formation of PKAhp8 could be a key element in DNA binding, not because of formation of more structured protein (which can be overestimated by FTIR, see above), but because of the incorporation of the phosphoryl

groups in the sequence. The introduced phosphoryl groups could make numerous electrostatic interactions and new hydrogen bonds when PKAhp8 binds to DNA; then, the entropic cost of folding would be largely compensated by the enthalpy of binding. A similar behavior has been observed in the binding of phosphorylated KID protein, to the protein KIX (31, 32).

It is important to note that in this work we have shown that the DNA binding affinity of hp8 is enhanced when it is PKA-phosphorylated, but we do not know whether the interaction with other biomolecule (or biomolecules) might also enhance its affinity to DNA. For instance, hp8 could bind DNA not only when it is PKA-phosphorylated but also when it binds to another biomolecule, as it happens in the transcriptional coactivator Bob 1 (33). Future studies must try to elucidate this possibility and identify other proteins interacting with hp8.

*p8 Is a HMG-I/Y-related Protein*—The detailed structural and biochemical analysis of the hp8 strongly suggests that it is a HMG-related protein, more particularly, a HMG-I/Y-related protein. In fact, although the identity between hp8 and HMG-I/Y is only around 35%, and the AT hook motif is not conserved, several other characteristics strongly support this presumption. For example, the similar molecular weight, isoelectric point, percentage of Arg + Lys, Glu + Asp, Ser + Thr, Gly + Pro, hydrophilicity plot, charge separation, and their high heat and TCA precipitation resistance. In addition, like HMG-I/Y proteins, hp8 is unstructured in solution and binds to DNA in a sequence-independent manner.

HMG proteins are abundant chromosome components, originally defined by their chemical properties and mobility on gels (34). Together with histones, they are the crucial components in the assembly of regulatory nucleoproteins complexes. Recently, a study has shown that HMG-I/Y is not essential for packaging DNA into chromosomes in the mouse (35), and a previous work established a similar status for vertebrates histone H1 (36), suggesting the presence of redundant functions in the chromatin higher ordered structure. However, HMG proteins seem to be essential for the transcription of several genes *in vivo* (35) and *in vitro* (37–40). In fact, HMG-I/Y was implicated in regulating the association of transcription factors with DNA. The presence of HMG-I/Y could improve the DNA binding of the transcription factors by helping DNA flexibility and thus stimulating transcription by severalfolds (reviewed in Ref. 41). In this way, it is interesting to note that mice null for p8 gene develop near to normality, indicating that this p8 (which has a high homology to hp8), like HMG-I/Y proteins, is not essential for chromatin organization; however, these mice show different patterns of gene expression in some tissues. Furthermore, p8 facilitates the Smads transcription activity in fibroblasts and strongly enhances the expression of the pancreatitis-associated proteins in pancreas with pancreatitis.<sup>2</sup>

*Acknowledgment*—We gratefully acknowledge Dr. F. Javier Gómez for discussions.

<sup>2</sup> A. Garcia-Montero, S. Vasseur, L. Giono, E. Cánepa, S. Moreno, J. C. Dagorn, and J. L. Iovanna, unpublished results.

## REFERENCES

- Mallo, G. V., Fiedler, F., Calvo, E. L., Ortiz, E. M., Vasseur, S., Keim, V., Morisset, J., and Iovanna, J. L. (1997) *J. Biol. Chem.* **272**, 32360–32369
- Vasseur, S., Mallo, G. V., Fiedler, F., Bödecker, H., Cánepa, E., Moreno, S., and Iovanna, J. L. (1999) *Eur. J. Biochem.* **259**, 670–675
- Jiang Y. F., Vaccaro M. L., Fiedler F., Calvo E. L., and Iovanna J. L. (2000) *Biochem. Biophys. Res. Commun.* **260**, 686–690
- Ree, A. H., Tvermyr, M., Engebraaten, O., Rooman, M., Røsek, Ø., Hovig, E., Meza-Zepeda, L. A., Bruland, Ø. S., and Fodstad, Ø. (1999) *Cancer Res.* **59**, 4675–4680
- Ree, A. H., Pacheco, M. M., Tvermyr, M., Fodstad, Ø., and Brentani, M. M. (2000) *Clin. Cancer Res.* **6**, 1778–1783
- Ferrer-Montiel, A. V., Montal, M. S., Diaz-Muñoz, S., and Montal, M. (1991) *Proc. Natl. Acad. Sci. U. S. A.* **88**, 10213–10217
- Zurdo, J., Sanz, J. M., González, C., Rico, M and Ballesta, J. P. G. (1997) *Biochemistry* **36**, 9625–9635
- Echabe, I., Encinar, J. A., and Arrondo, J. L. R. (1997) *Biospectroscopy* **3**, 469–475
- Fernández-Ballester, G., Castresana, J., Arrondo, J. L. R., Ferragut, J. A., and González-Ros, J. M. (1992) *Biochem. J.* **288**, 421–426
- Moffat, D. J., and Mantsch, H. H. (1992) *Methods Enzymol.* **210**, 192–200
- Surewicz, W. K., Mantsch, H. H., and Chapman, D. (1993) *Biochemistry* **32**, 389–394
- Bañuelos, S., Arrondo, J. L. R., Goñi, F. M., and Pifat, G. (1995) *J. Biol. Chem.* **270**, 9192–9196
- Moffat, D. J., Kaupinnen, J. K., Cameron, D. G., Mantsch, H. H., and Jones, R. N. (1986) *Computer Programs for Infrared Spectroscopy, NHCC Bulletin*, Vol. 18, National Research Council of Canada, Ottawa, Canada
- Encinar, J. A., Fernández, A. M., Dasgupta, B. R., Ferragut, J. A., Montal, M., González-Ros, J. M., and Ferrer-Montiel, A. M. (1998) *FEBS Lett.* **429**, 78–82
- Bustin, M., and Reeves, R. (1996) *Prog. Nucleic Acids Res. Mol. Biol.* **54**, 35–100
- Creighton, T. (1993) *Proteins: Structures and Molecular Properties*, 2nd Ed., W. H. Freeman and Co., New York
- Johnson, W. C. Jr. (1988) *Annu. Rev. Biophys. Biophys. Chem.* **17**, 145–166
- Woody, R. W. (1995) *Methods Enzymol.* **246**, 34–71
- Jackson, M., and Mantsch, H. H. (1995) *Crit. Rev. Biochem. Mol. Biol.* **30**, 95–120
- Braiman, M. S., and Rothschild, K. J. (1988) *Annu. Rev. Biophys. Biophys. Chem.* **17**, 541–570
- Arrondo, J. L. R., Mantsch, H. H., Mullner, N., Pikula, S., and Martonosi, A. (1987) *J. Biol. Chem.* **262**, 9037–9043
- Krimm, S., and Bandekar, J. (1986) *Adv. Prot. Chem.* **38**, 181–364
- Allain, F. H. T., Yen, Y.-M., Masse, J. E., Schultze, P., Dieckmann, T., Johnson, R. C., and Feigon, J. (1999) *EMBO J.* **18**, 2563–2579
- Wüthrich, K. (1986) *NMR of Proteins and Nucleic Acids*, John Wiley & Sons, New York
- Sánchez-Ruiz, J. M., and Martínez-Carrión, M. (1988) *Biochemistry* **27**, 3338–3342
- Byler, D. M., and Susi, H. (1986) *Biopolymers* **25**, 469–487
- Jones, B. E., Dossonet, V., Küster, E., Hillen, W., Deutscher, J., and Kleit, R. E. (1997) *J. Biol. Chem.* **272**, 26530–26535
- Buck, M. (1998) *Q. Rev. Biophys.* **31**, 297–355
- Thomas, P. D., and Dill, K. A. (1993) *Protein Sci.* **2**, 2050–2065
- Weiss, M. A., Ellenberger, T., Wobbe, C. R., Lee, J. P., Harrison, S. C., and Struhl, K. (1990) *Nature* **347**, 575–578
- Wright, P. E., and Dyson, H. J. (1999) *J. Mol. Biol.* **293**, 321–331
- Radhakrishnan, I., Pérez-Alvarado, G. C., Parker, D., Dyson, H. J., Montminy, M. R., and Wright, P. E. (1997) *Cell* **91**, 741–752
- Chang, J-F, Phillips, K., Lundback, T., Gstaiger, M., Ladbury, J. E., and Luisi, B. (1999) *J. Mol. Biol.* **288**, 941–952
- Grosschedl, R., Giese, K., and Pagel, J. (1994) *Trends Genet.* **10**, 94–100
- Calogero S., Grassi F., Aguzzi A., Voigtlander T., Ferrier P., Ferrari S., and Bianchi M. E. (1999) *Nat. Genet.* **22**, 276–280
- Ohsumi, K., Katagiri, C., and Kishimoto T. (1993) *Science* **262**, 2033–2035
- Ge, H., and Roeder, R. G. (1994) *J. Biol. Chem.* **269**, 17136–17140
- Zappavigna V., Falciola, L., Citterich, M. H., Mavilio, F., and Bianchi, M. E. (1996) *EMBO J.* **15**, 4981–4991
- Boonyaratanakornkit V., Melvin V., Prendergast P., Altmann M., Ronfani L., Bianchi M. E., Taraseviciene L., Nordeen S. K., Allegretto E. A., and Edwards D. P. (1998) *Mol. Cell. Biol.* **18**, 4471–4487
- Sutrias-Grau, M., Bianchi, M. E., and Bernues, J. (1999) *J. Biol. Chem.* **274**, 1628–1634
- Bianchi M. E., and Beltrame M. (1998) *Am. J. Hum. Genet.* **63**, 1573–1577